QPSK-to-2×BPSK wavelength and modulation format conversion through phase-sensitive four-wave mixing in a highly nonlinear optical fiber

Da Ros, Francesco; Dalgaard, Kjeld; Lei, Lei; Xu, Jing; Peucheret, Christophe

Published in:
Optics Express

Link to article, DOI:
10.1364/OE.21.028743

Publication date:
2013

Document Version
Publisher's PDF, also known as Version of record

QPSK-to-2×BPSK wavelength and modulation format conversion through phase-sensitive four-wave mixing in a highly nonlinear optical fiber

Francesco Da Ros,[1,*] Kjeld Dalgaard,[1] Lei Lei,[1,2] Jing Xu,[1] and Christophe Peucheret[1]

[1]*Department of Photonics Engineering, Technical University of Denmark, 2800 Kgs. Lyngby, Denmark*

[2]*Wuhan National Laboratory for Optoelectronics, School of Optoelectronics Science and Engineering, Huazhong University of Science and Technology, Wuhan, 430074, Hubei, China*

[*]*fdro@fotonik.dtu.dk*

Abstract: A phase-sensitive four-wave mixing (FWM) scheme enabling the simultaneous conversion of the two orthogonal quadratures of an optical signal to different wavelengths is demonstrated for the first time under dynamic operation using a highly nonlinear optical fiber (HNLF) as the nonlinear medium. The scheme is first optimized with respect to the power levels and phases of the four phase-coherent pumps. The successful modulation and wavelength conversion of the two complex quadratures of a quadrature phase-shift keying (QPSK) signal to two binary phase-shift keying (BPSK) signals is then demonstrated experimentally with no power penalty at a bit-error-ratio (BER) of 10^{-9} compared to direct interferometric demodulation of the QPSK signal.

OCIS codes: (060.5060) Phase modulation; (070.4340) Nonlinear optical signal processing; (190.4380) Nonlinear optics, four-wave mixing.

References and links

1. R. Slavík, F. Parmigiani, J. Kakande, C. Lundström, M. Sjödin, P. A. Andrekson, R. Weerasuriya, S. Sygletos, A. D. Ellis, L. Grüner-Nielsen, D. Jakobsen, S. Herstrøm, R. Phelan, J. O'Gorman, A. Bogris, D. Syvridis, S. Dasgupta, P. Petropoulos, and D. J. Richardson, "All-optical phase and amplitude regenerator for next-generation telecommunications systems," Nat. Photonics **4,** 690-695 (2010).
2. Z. Tong, C. Lundström, P. A. Andrekson, C. J. McKinstrie, M. Karlsson, D. J. Blessing, E. Tipsuwannakul, B. J. Puttnam, H. Toda, and L. Grüner-Nielsen, "Towards ultrasensitive optical links enabled by low-noise phase-sensitive amplifiers," Nat. Photonics **5**, 430–436 (2011).
3. J. Kakande, A. Bogris, R. Slavík, F. Parmigiani, D. Syvridis, P. Petropoulos, and D. J. Richardson, "First demonstration of all-optical QPSK signal regeneration in a novel multi-format phase sensitive amplifier," in *European Conference on Optical Communication* (2010), postdeadline paper 3.3.
4. T. Richter, R. Elschner, and C. Schubert, "QAM phase-regeneration in a phase-sensitive fiber-amplifier,", in *European Conference on Optical Communication* (2013), paper We.3.A.2.
5. R.P. Webb, J.M. Dailey, R.J. Manning, and A.D. Ellis, "Phase discrimination and simultaneous frequency conversion of the orthogonal components of an optical signal by four-wave mixing in an SOA," Opt. Express **19,** 20015–20022 (2011).
6. R.P. Webb, M. Power, and R.J. Manning, "Phase-sensitive frequency conversion of quadrature modulated signals," Opt. Express **21,** 12713–12727 (2013).

#195804 - $15.00 USD Received 14 Aug 2013; revised 24 Oct 2013; accepted 31 Oct 2013; published 14 Nov 2013

7. L. K. Oxenløwe, A. Clausen, M. Galili, H. C. Hansen Mulvad, H. Ji, H. Hu, and E. Palushani, "Ultra-high-speed optical time division multiplexing", in *Optical Fiber Telecommunications VIA*, I. P. Kaminow, T. Li and A. E. Willner Eds (Academic Press, Oxford, 2013).
8. F. Da Ros, P. M. Calabrese, N. Kang, E. Palushani, and C. Peucheret, "Orthogonal phase quadratures conversion to different wavelengths through phase-sensitive four-wave mixing in an highly nonlinear fiber," in *Optical Fiber Communication Conference*, OSA Technical Digest (Optical Society of America, 2013), paper OW4C-3.
9. M. Gao, T. Kurosu, T. Inoue, and S. Namiki, "Low-penalty phase de-multiplexing of QPSK signal by dual pump phase sensitive amplifiers," in *European Conference on Optical Communication* (2013), paper We.3.A.5.
10. B. P.-P. Kuo, J. M. Fini, L. Grüner-Nielsen, and S. Radic, "Dispersion-stabilized highly-nonlinear fiber for wide-band parametric mixer synthesis," Opt. Express **20,** 18611–18619 (2012).
11. R. Slavík, J. Kakande, and D. J. Richardson, "Practical issues and some lessons learned from realization of phase sensitive parametric regenerators," in *Optical Fiber Communication Conference*, OSA Technical Digest (Optical Society of America, 2012), paper OW3C-4.
12. F. Da Ros, J. Xu, L. Lei and C. Peucheret, "Phase noise tolerant QPSK receiver using phase sensitive wavelength conversion," in *OptoElectronics and Communications Conference/Photonics in Switching* (2013), paper TuS2-5.
13. M. Seimetz, *High-Order Modulation for Optical Fiber Transmission* (Springer, Berlin, 2009).

1. Introduction

Phase-sensitive all-optical signal processing has received a significant interest in recent years, leading to several breakthroughs being reported spanning from binary phase-shift keying (BPSK) regeneration [1] to low noise amplification [2]. Meanwhile, in order to satisfy the ever increasing demand for capacity, optical communication systems are constantly migrating towards higher order modulation formats such as quadrature phase-shift keying (QPSK) and quadrature amplitude modulation (QAM), enabling an improvement in the spectral efficiency. Therefore, an important requirement for all-optical phase-sensitive processing is the scalability towards such modulation formats. Along this direction, various schemes have been proposed and experimentally demonstrated to enable the phase regeneration of QPSK [3] and of 8-QAM [4] signals.

Recently, R. P. Webb *et al*. have proposed to use phase-sensitive four-wave mixing (FWM) between a signal and four phase-coherent pumps to all-optically separate the two complex quadratures of the signal by converting them to different wavelengths [5]. They have also demonstrated experimentally such a scheme under static (i.e. employing continuous wave (CW) pumps and signal) operation using semiconductor optical amplifiers (SOAs) as nonlinear media. Even though the operation of the scheme was numerically predicted at a symbol rate as high as 40 Gbaud and positive conversion efficiencies have been reported with pump spacing of 600 GHz [6], signals processed by SOAs are more prone to be affected by pattern effects when operating at high bit rates due to a relatively slow carrier recovery time. To fully exploit the benefits of all-optical signal processing, bit rate transparent operation is a desirable condition. Among other nonlinear media, passive highly nonlinear optical fibers (HNLFs) have been extensively used for ultra-high speed all-optical processing [7]. We have recently shown that HNLFs also present a good potential for the implementation of quadrature-dependent wavelength conversion [8]. However, our experimental demonstration was so far limited to a static characterization.

In this article, we extend our previous work to dynamic operation and demonstrate QPSK-to-$2\times$BPSK simultaneous modulation format and wavelength conversion. The orthogonal quadratures of a 10-Gbaud QPSK signal are simultaneously converted to two 10-Gbps BPSK signals located at different wavelengths. Using two different data patterns for the in-phase ($DATA_I$) and quadrature ($DATA_Q$) components of the QPSK signal, we demonstrate the successful recovery of each quadrature pattern after phase-sensitive FWM wavelength conversion to two different idlers and demodulation by a 1-bit delay interferometer (DI) followed by balanced detection. Furthermore, we show that the two converted quadratures can be recovered error-free (i.e. with a bit-error-ratio (BER) better than 10^{-9}) with negligible power penalty compared

#195804 - $15.00 USD Received 14 Aug 2013; revised 24 Oct 2013; accepted 31 Oct 2013; published 14 Nov 2013

to standard demodulation of a differential QPSK (DQPSK) signal using a 1-symbol DI and balanced detection. In contrast with another recently demonstrated phase-sensitive technique allowing phase demultiplexing of a QPSK signal where one single idler was generated [9], the method used in the present work enables simultaneous recovery of the two BPSK quadratures.

The remaining of this article is organized as follows. The operation principle of the scheme is described in Section 2. Section 3 introduces the main blocks of the experimental setup used for both the static characterization (Section 4) and the system experiment (Section 5). Finally the results are discussed in Section 6 and the conclusions are drawn in Section 7.

2. Operation principle

The demonstrated converter relies on the use of four phase-coherent CW pumps (denoted as *P*1-*P*4) that are injected together with a phase-coherent signal (denoted as *S*) into an HNLF, as illustrated in Fig. 1. Phase-sensitive FWM in the fiber enables the generation of two idlers (denoted as *I* and *Q*), whose conversion efficiencies with respect to the input signal are determined by the phase relation between signal and pumps. In this work, the conversion efficiencies are defined as the ratio of the idler powers at the HNLF output to the signal power at its input. By optimizing the pumps phases and power levels together with the signal power, the conversion efficiency versus signal phase responses of the two idlers can be phase-shifted by 90°, enabling the conversion of the in-phase and quadrature components of *S* to *I* and *Q*, respectively. This effect can be more clearly seen by looking at the output idlers phases as a function of the input signal phase. The 90° shifted two-level curves indeed enable such a conversion.

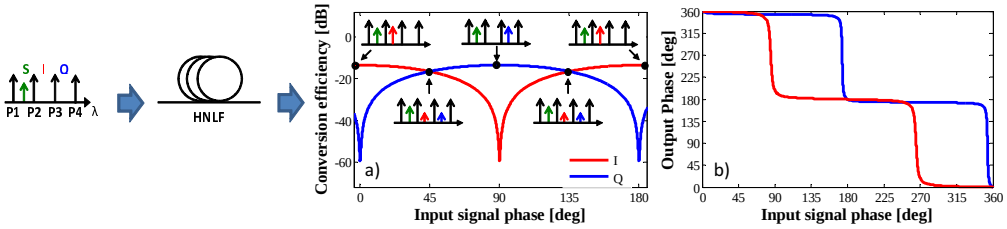

Fig. 1. Operation principle sketching the waves allocation at the input and output of the HNLF together with the conversion efficiencies and output phases for the two idlers (*I* and *Q*) as a function of the input signal phase. The curves have been obtained through numerical simulations.

Other than the desired 90° phase-shift, it is also critical to provide a high value of phase-sensitive extinction ratio (ER). The flatness of the output idler phase versus input signal phase response is strongly related to the ER of the conversion efficiency versus input signal phase response. Therefore, in order to minimise the transfer of phase noise from the input signal to the two idlers, a high phase-sensitive ER should be obtained.

Figure 1 shows the results of a numerical optimization carried out using optimization routines provided by MATLAB® combined with the conventional split-step Fourier method to solve the nonlinear Schrödinger equation describing the waves propagation in the HNLF. The parameters used to model the HNLF follow the parameters of the fiber used in the experiment and are listed in Section 5.

It should be noted that, in the numerical simulations, the power per pump coupled into the HNLF has been kept below the stimulated Brillouin scattering (SBS) threshold (around 17 dBm for the HNLF used in this work), in order to neglect backscattering effects. In practice, SBS represents one of the main limitations to increasing the conversion efficiency for the two idlers. However, several SBS mitigation methods such as fiber straining [10] have the potential to

#195804 - $15.00 USD Received 14 Aug 2013; revised 24 Oct 2013; accepted 31 Oct 2013; published 14 Nov 2013

increase the achievable conversion efficiency. In our experiment, a standard HNLF was used as the obtained conversion efficiencies were sufficient to achieve error-free performances.

3. Experimental setup

A block diagram of the experimental setup is shown in Fig. 2. The four pumps and the signal are generated from a single CW laser source by frequency comb generation using phase modulation by a single tone radio-frequency signal with a high modulation index. Frequency comb generation is used to guarantee a stable phase relation between the five waves involved in the phase-sensitive process. For practical applications where the pumps would be generated at the processing stage, frequency comb generation exploiting some phase recovery scheme such as the one described in [1] could be employed. Alternatively, the phase coherence could be created through an additional FWM pre-stage as discussed in [11].

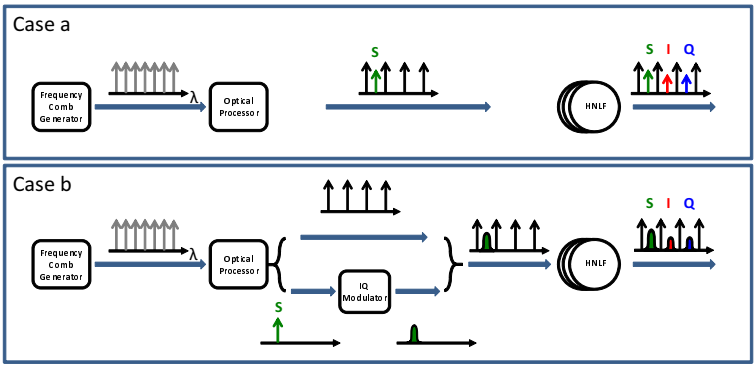

Fig. 2. Block diagrams of the experimental setup: static characterization (case a) and system experiment (case b).

An optical processor (Finisar Waveshaper) is then used to select four CW pumps separated by 80 GHz and a CW signal located in-between the shortest wavelength pumps. For the static characterization (case a), all the selected waves have been directed towards the same output port of the processor, therefore injecting into the HNLF five CW signals. For the system experiment (case b), the signal was sent to a different port, QPSK-modulated, recombined with the four pumps and injected into the HNLF. At the fiber output the two idlers are generated in the empty slots between the pumps, *I* and *Q* being either two CW signals (case a) or two BPSK signals (case b).

4. Static characterization

In order to meet the two fundamental requirements for the scheme, i.e. a 90° shift between the idlers conversion efficiency versus signal phase responses, and a sufficient phase-sensitive ER, the power levels and phases of the four pumps have been optimized together with the signal power by use of the optical processor. Starting from the results of the numerical optimization, the nine optimisation parameter values have been fine tuned experimentally, leading to the conversion efficiencies reported in Fig. 3 together with the spectra at the HNLF output for three different values of the signal phase.

The conversion efficiency curves show the desired phase shift and ERs in excess of 13 dB. These results have been obtained for the power levels at the HNLF input and relative phases between the waves reported in Table 1.

#195804 - $15.00 USD Received 14 Aug 2013; revised 24 Oct 2013; accepted 31 Oct 2013; published 14 Nov 2013

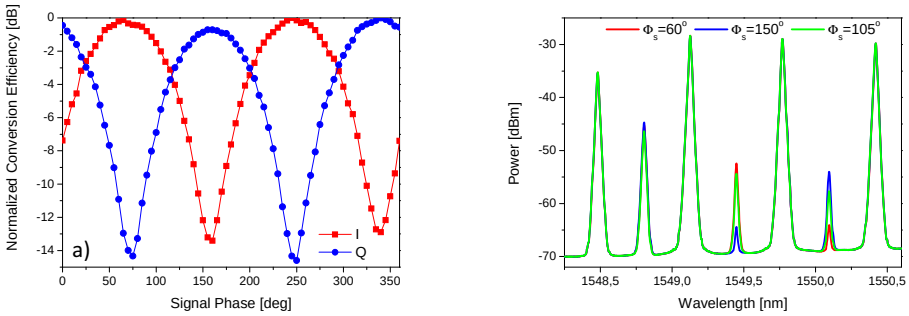

Fig. 3. (a) Conversion efficiencies for I and Q as a function of the input signal phase. (b) Spectra measured at the HNLF output for three values of the signal phase showing the maximum amplification for I ($\Phi_s = 60°$) and Q ($\Phi_s = 150°$), as well as the quadrature point ($\Phi_s = 105°$) where the idlers output powers are 3 dB below their maximum.

Table 1. Experimental optimization results: power levels and phases of the five waves at the HNLF input. The phase of the signal is swept in order to produce the phase-dependent wavelength conversion curves.

	Pump 1	Pump 2	Pump 3	Pump 4	Signal
Power [dBm]	6.9	14.3	14.7	12.5	-2.5
Phase [rad]	1.1	0.3	1.4	0.1	-

5. System experiment

A continuous wave signal emitted at 1550 nm by a narrow linewidth (∼100 kHz) external cavity tunable laser source (TLS) was phase modulated (PM) with a 40-GHz radio frequency signal with a modulation index (defined as the ratio of the peak-to-peak voltage of the driving signal to the half-wave voltage of the phase modulator) of 4.3 in order to generate an optical frequency comb with 40-GHz line spacing (Fig. 4).

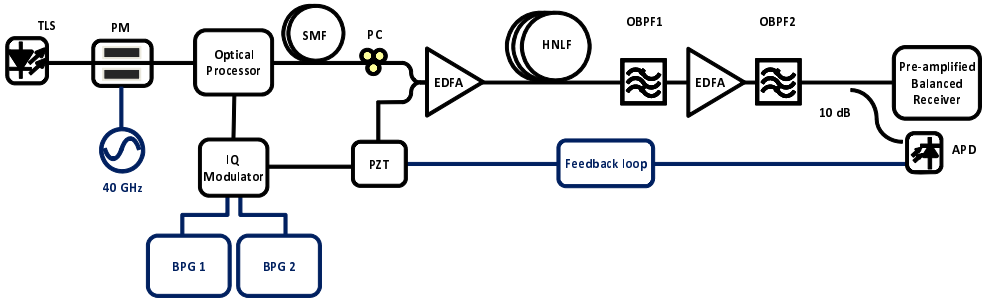

Fig. 4. Experimental setup for dynamic phase-sensitive wavelength and format conversion of a 10-Gbaud QPSK signal.

The optical processor was used to select four 80-GHz spaced pumps and a signal out of the frequency comb and to adjust their power levels and relative phases according to the values reported in Table 1. It was also used to separate the signal from the pumps by outputting it to a different port so that it could be modulated in the QPSK format at 10 Gbaud using a standard IQ modulator driven by two non return-to-zero signals at 10 Gbps carrying two different pseudo-random binary sequences (PRBSs) coming from two independent bit pattern generators (BPGs)

#195804 - $15.00 USD Received 14 Aug 2013; revised 24 Oct 2013; accepted 31 Oct 2013; published 14 Nov 2013

synchronized with a common reference signal at 10 GHz. The pumps were propagated through 10 m of standard single mode fiber (SMF) and coupled back together with the signal via a 3-dB coupler. The length of SMF has been optimized in order to approximately match the pumps and signal path lengths in order to ease the operation of the phase control loop aiming at compensating for slow thermal drifts. A polarization controller (PC) was used to align the state of polarization of the pumps to the that of the signal in order to maximize the FWM efficiency.

The five waves were then amplified to 19 dBm of total power at the fiber input with an erbium-doped fiber amplifier (EDFA) and injected into a 500-m long HNLF with zero-dispersion wavelength of 1550.4 nm, dispersion slope of 0.0185 ps/(nm^2·km), loss of 0.7 dB/km and nonlinear coefficient of 10.7 W^{-1}·km^{-1}. At the fiber output, a pair of optical bandpass filters (OBPFs) with 0.8 and 0.3-nm full-width at half-maximum bandwidths, were used to select one of the idlers at a time and input it to the pre-amplified BPSK balanced receiver for BER testing. A second EDFA located between the OBPFs was used to compensate for their insertion losses. Finally, phase-to-intensity demodulation in the receiver was performed by a 1-bit (100 ps) delay interferometer followed by a balanced photodiode with cut-off frequency of 45 GHz.

The splitting of pumps and signal and their propagation along different paths inevitably results in a loss of phase coherence due to thermal effects, even when balancing the paths lengths. In order to lock the waves in phase, 10% of the selected idler power was detected by a slow speed avalanche photodiode (APD) and used as reference for a feedback loop based on a piezoelectric actuator (PZT). The PZT has a bandwidth of 15 kHz and therefore is able to compensate for the slow thermal drift between the waves.

The phase stabilization mechanism relies on tracking the average power variations of one of the idlers as the relative phase between signal and pumps drifts. The phase sensitive FWM directly maps the phase drifts into power variations of the idlers. For instance, applying a low frequency (below 10 kHz) linear phase modulation to the signal through the PZT, the average powers of the idlers detected through the APD (50 MHz 3-dB bandwidth) varies according to the sine square transfer functions reported in Fig. 3(a). As both the APD and PZT are narrow bandwidth, the fast phase variations due to the 10-Gbaud modulation are averaged out and cannot be detected by the scheme.

Furthermore, it is critical to rotate the common phase of the QPSK signal such that the constellation points match the quadrature points of the conversion efficiency versus input signal phase curves, i.e. the points where the output phase is constant in Fig. 1. As the minima in conversion efficiency correspond to sharp 180° phase transitions, the constellations points need to be equally distant from such minima to avoid an increase in phase noise as discussed in [12]. Also, and more importantly, aligning the constellation to match the position of the maxima and minima in the CE curve would lead to phase-to-intensity modulation conversion, and the idlers would then be modulated in the on-off keying (OOK) format. In such a scenario, the information carried by both idlers would be the result of exclusive OR operation between $DATA_I$ and $DATA_Q$, with consequent loss of information. The stabilization scheme therefore locks the idler power to the quadrature point of the conversion efficiency, i.e. 3 dB below the maximum, for optimal performances.

It has also been ensured that the phase stabilization mechanism would allow for independent detection of the two idlers. Phase-locking based on the power of one of the idlers enables to recover the information of either idler without requiring additional tuning of the feedback system.

#195804 - $15.00 USD Received 14 Aug 2013; revised 24 Oct 2013; accepted 31 Oct 2013; published 14 Nov 2013

6. Results

The spectra of the frequency comb, together with those recorded at the input and output of the HNLF are shown in Fig. 5. The existence of two modulated idlers is clearly confirmed in the output spectrum.

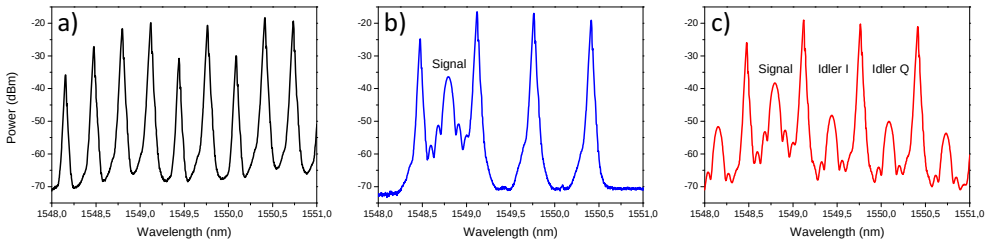

Fig. 5. Optical spectra: (a) frequency comb, (b) input (showing the four pumps and the input QPSK signal) and (c) output in phase-locking operation (showing the generated BPSK idlers) of the HNLF.

In order to verify the successful conversion of the two quadratures of the QPSK signal to different wavelengths, two different sequences have been applied to the inputs of the IQ modulator, i.e. a PRBS of length $2^7 - 1$ for $\mathrm{DATA_I}$ and a PRBS of length $2^9 - 1$ for $\mathrm{DATA_Q}$. A digital sampling oscilloscope was then used at the receiver to save 50 bits demodulated from each idler, indeed proving that I was carrying $\mathrm{DATA_I}$ while $\mathrm{DATA_Q}$ could be retrieved from Q. The electrical waveforms after interferometric demodulation and balanced detection are shown in Fig. 6, together with the binary values of the corresponding PRBSs, showing that indeed the data carried by the phases of the generated idlers match the original PRBSs modulated on each quadrature of the QPSK signal. The thickness of the recorded oscilloscope traces are partly caused by a sub-optimum phase stabilization loop which does not fully and instantaneously compensate for the phase drifts.

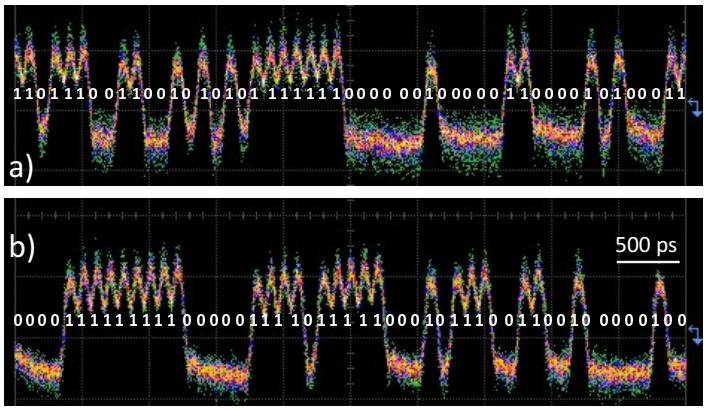

Fig. 6. Temporal waveforms saved by a digital sampling oscilloscope at the receiver side after interferometric demodulation and balanced detection for (a) I (corresponding to a $2^7 - 1$ PRBS) and (b) Q (corresponding to a $2^9 - 1$ PRBS).

The performances of the two converted idlers have been evaluated through BER measurements. In these measurements, decorrelated PRBSs of length $2^{15} - 1$ have been used as $\mathrm{DATA_I}$ and $\mathrm{DATA_Q}$. The results of BER measurements as a function of the average received power

#195804 - $15.00 USD Received 14 Aug 2013; revised 24 Oct 2013; accepted 31 Oct 2013; published 14 Nov 2013

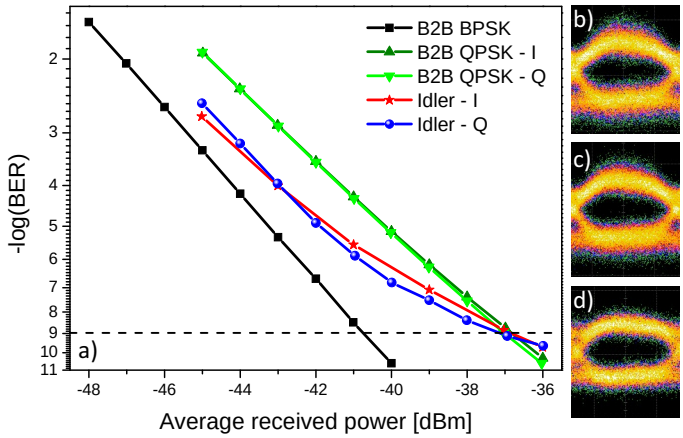

Fig. 7. (a) BER performances for the converted idlers together with back-to-back QPSK and BPSK as references. Eye diagrams for (b) *I*, (c) *Q* and (d) one quadrature of the demodulated back-to-back QPSK signal for a received power of −35 dBm and 10 s of acquisition time.

are shown in Fig. 7 and compared with back-to-back performances for both a BPSK signal at 10 Gbps and a QPSK signal at 10 Gbaud. The reference BPSK signal was demodulated using the 100-ps DI while, for the reference QPSK, the two quadratures were demodulated one at a time using the same 100-ps DI and tuning the bias point of the DI to different values. It should be noted that, for the back-to-back QPSK quadratures, the demodulated signal is no longer a simple PRBS (as were the original $DATA_I$ and $DATA_Q$), since no differential encoding had been applied at the transmitter [13]. Instead the error analyzer was programmed with the expected patterns.

A comparison between the detected BPSK idlers and the demodulated back-to-back QPSK signal shows a sensitivity improvement above 1.5 dB at a BER of 10^{-3} and equal performances at a BER of 10^{-9}. The slight tilt of the BER curves for the idlers at high received power is partly caused by the sub-optimum stabilization which leads to more severe impairments as the gating time needed to obtain a reliable error counting gets longer. Nevertheless clear and open eye diagrams can be seen. A power penalty of about 4 dB is measured for the converted idlers compared to the simple case of BPSK modulation and interferometric detection.

7. Conclusion

We have demonstrated simultaneous QPSK-to-2×BPSK modulation format and wavelength conversion using phase-sensitive FWM in an HNLF. The scheme has been numerically and experimentally optimized achieving phase-sensitive ERs in excess of 13 dB for both idlers. The conversion of both complex quadratures $DATA_I$ and $DATA_Q$ of a 10-Gbaud QPSK signal to two distinct BPSK idlers *I* and *Q* has been experimentally demonstrated, reporting error-free performances (BER 10^{-9}) with no power penalty compared to the detection of the QPSK signal using a 1-symbol delay interferometer.

Acknowledgments

The authors are grateful to V. Cristofori and M. Galili for their comments and suggestions. This work was supported by the Danish Research Council for Technology and Production Sciences (project 09-066562). OFS Fitel Denmark is acknowledged for providing the HNLF.